

# New Perspective on Progressive GANs Distillation for One-class Novelty Detection

Zhiwei Zhang, Yu Dong, Hanyu Peng, Shifeng Chen

**Abstract**—One-class novelty detection is conducted to identify anomalous instances, with different distributions from the expected normal instances. In this paper, the Generative Adversarial Network based on the Encoder-Decoder-Encoder scheme (EDE-GAN) achieves state-of-the-art performance. The two factors below serve the above purpose: 1) The EDE-GAN calculates the distance between two latent vectors as the anomaly score, which is unlike the previous methods by utilizing the reconstruction error between images. 2) The model obtains best results when the batch size is set to 1. To illustrate their superiority, we design a new GAN architecture (ED $\hat{E}$ -GAN), and compare performances according to different batch sizes. Moreover, with experimentation leads to discovery, our result implies there is also evidence of just how beneficial constraint on the latent space are when engaging in model training.

In an attempt to learn compact and fast models, we present a new technology, Progressive Knowledge Distillation with GANs (P-KDGAN), which connects two standard GANs through the designed distillation loss. Two-step progressive learning continuously augments the performance of student GANs with improved results over single-step approach. Our experimental results on CIFAR-10, MNIST, and FMNIST datasets illustrate that P-KDGAN improves the performance of the student GAN by 2.44%, 1.77%, and 1.73% when compressing the computation at ratios of 24.45:1, 311.11:1, and 700:1, respectively.

**Index Terms**—Novelty detection, generative adversarial network, knowledge distillation

## I. INTRODUCTION

One-class novelty detection (ND) aims to identify patterns that do not belong to the normal data distribution [6], [28], [37]. ND has a wide variety of applications such as network intrusion [11], credit card fraud [46], video surveillance [31], [22], [26], [17], medical diagnoses [44] and many more [30], [29], [54]. Unlike the traditional classification problem, ND methods operate on the assumption deemed to be semi-supervised that they are trained on normal samples only, while testing is carried out on a set of normal and outlier-class samples [23], [7], [42]. Currently, novelty detection methods can be divided into two categories according to their experimental setting. The first category methods regard single class as Inlier, and multiple classes as Outlier (termed “SIMO”) [5], [40], [12], [47], [1], [36], [13], [41]. In contrast, the second category methods treat multiple classes as Inlier,

This manuscript is an extended version of the published paper, *P-KDGAN: Progressive Knowledge Distillation with GANs for One-class Novelty Detection, IJCAI 2020*, and is being submitted to IEEE Transactions on Image Processing for peer review, September 15, 2021

Zhiwei Zhang, Yu Dong, Hanyu Peng, and Shifeng Chen are with Center for Multimedia Integrated Technologies, Shenzhen Institutes of Advanced Technology, Chinese Academy of Sciences, Shenzhen 518055, China. Shifeng Chen is the corresponding author: shifeng.chen@siat.ac.cn.

and single class as Outlier (called “MISO”) [4], [2], [48], [50], [27], [3]. In this paper, we focus on dealing with the former “SIMO” problems.

With the advantage of deep learning, novelty detection based on generative adversarial networks (GANs) has shown state-of-the-art performance by learning the representative latent space of high-dimensional data [44], [57], [43], [2], [3]. The previous methods can be roughly divided into two categories based on using different anomaly score. The former methods use the residual loss between input and reconstructed images as anomaly score [44], [57], [43]. Fast AnoGAN [43] used the loss in the latent space for training, but did not use it as an anomaly score during inference. The above anomaly score based on pixel-to-pixel image matching is less robust to noises, which can be proved in our comparative experiments. The latter methods, such as Ganomaly [2] and Skip-Ganomaly [3], used the residual loss between two latent vectors (Figure 4 (c)) on “MISO” tasks and achieved significant improvement. In this paper, we firstly utilize the EDE-GAN (Generative Adversarial Network based on Encoder-Decoder-Encoder architecture) model on “SIMO” task and achieves state-of-the-art performance when the batch size is set to 1. Previous works ignored an important factor, the impact of batch size in Batch Normalization (BN) [16] on the performance of one-class novelty detection. Different from traditional classification tasks, training data for one-class ND has only one category. In this paper, we would like to explain the influence of the batch size on one-class ND based on the following two points. 1) Model Fitting. As we know, BN is based on different channels to model all samples in a batch by calculating their mean and variance, assuming a normal distribution. If the batch size is larger than 1, the model’s ability to fit each sample will be weakened. 2) Generalization. The smaller batch size, meaning the larger gradient noise, impacts the generalization of model, and the results in Figure 1 demonstrate it well. In addition, we design a new GAN architecture (Figure 4 (b), ED $\hat{E}$ -GAN) and perform comparative experiments to demonstrate the effectiveness of the constraint on the latent space.

However, deep neural networks with high computational costs and large storage prohibit their deployment to computation and memory resource limited systems. For tackling the above issue, neural network compression has been widely applied in recent years [8], [34], [35]. As one of the mainstream compression methods, Knowledge Distillation (KD) following a teacher-student paradigm transfers knowledge from a teacher network with higher performance to a student network. The early contributions used the outputs of

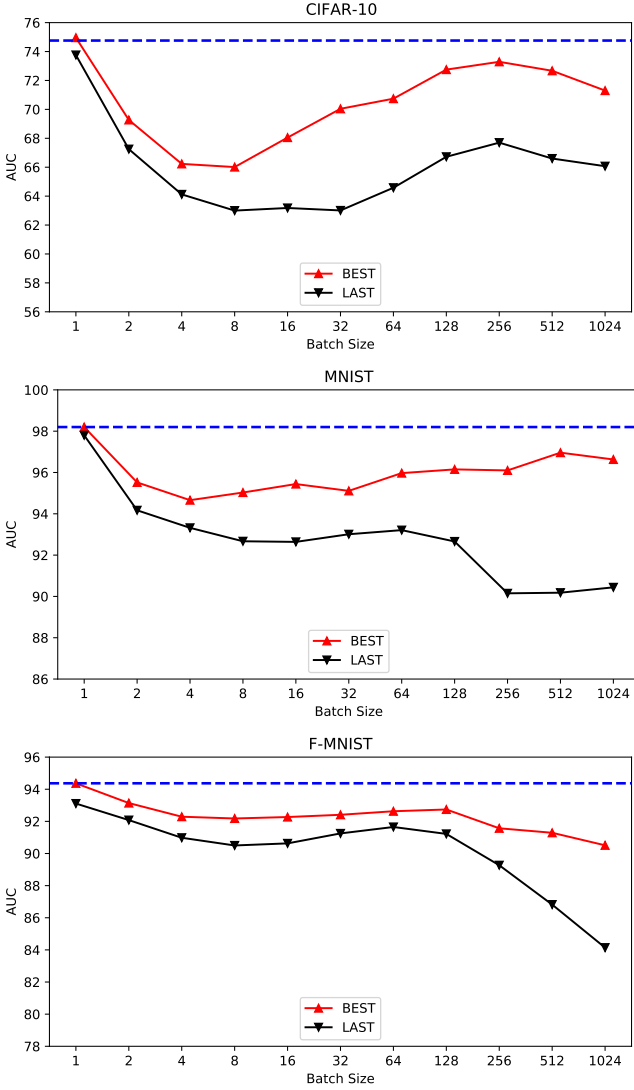


Fig. 1: The AUC of EDE-GAN model on varying batch sizes. When  $B=1$ , the model achieves the best performance on three datasets, which is contrary to the traditional classification problem. “BEST” represents the best result over all training epochs, “LAST” denotes the performance in the last training epoch.

the softmax layers or intermediate layers in teacher networks to improve the performance of student networks [15], [39]. In the later researches, the adversarial loss was proposed to evaluate the distinction between the distribution spaces of teacher and student networks [51], [52], [25], [14]. To our knowledge, there are no related works on two standard GANs [14] including two generators and two discriminators to design the distillation loss for knowledge distillation. Additionally, there are rare works investigating the initialization of student networks while random initialization is common used. Our experiments demonstrate that student networks without “knowledge” reserve (with random initialization) do not mimic the outputs of teacher networks well.

In this paper, we apply EDE-GAN for one-class novelty detection that outperforms the state-of-the-art approaches. In

order to deploy the deep neural networks in computation resources limited mobile devices, we propose the Progressive Knowledge Distillation with GANs (P-KDGAN) method to train the lightweight student network. The P-KDGAN approach improves the performance of student GAN by solving the following three problems. 1) How to design a distillation loss to measure the similarity of intermediate representations learned from the teacher GAN and the student GAN? The distillation loss  $K_l$  described in Eq.7 is designed as the weighted sum of the losses  $K_1$ ,  $K_x$  and  $K_2$ . 2) As shown in Figure 3 (b), how to combine the distillation loss  $K_l$  with existing generator losses  $L_g^S$ ,  $L_g^T$  and discriminator losses  $L_d^S$ ,  $L_d^T$  from the student and teacher GANs to improve the performance of the student GAN? As is illustrated in Figure 3(b), we design four distillation structures based on different combinations of the above five losses. 3) Whether the designed four distillation structures can make the performance of the student GAN like that of the teacher GAN? If not, how to fix it? Our experimental results demonstrate that the performance of student GANs trained from scratch (or with random initialization) by the above four distillation structures is incomparable with the teacher GAN. Just as learning is a gradual cumulative process, a two-step progressive learning of KDGAN is proposed to continuously improve the performance of the student GAN. The detailed solutions will be illustrated in Section III.

The performance of proposed progressive knowledge distillation on GANs for one-class novelty detection is evaluated on CIFAR-10 [20], MNIST [21] and FMNIST [56] datasets. Our contributions are summarized as follows.

- We utilize the EDE-GAN for one-class novelty detection, which outperforms the state-of-the-art methods. We also design a new GAN architecture and perform comparative experiments to demonstrate the influence of the batch size and the effectiveness of the constraint on the latent space.
- We propose new distillation losses on latent vectors and reconstructed images of GANs to transfer knowledge from the teacher to student network. The distillation process is regarded as a knowledgeable teacher to improve the performance and stability of students through a two-step progressive learning, which includes basic knowledge learning and fine-learning.
- Progressive Knowledge Distillation with GANs is proposed for one-class novelty detection. Our experiments demonstrate that the P-KDAGN can improve the performance of the student GAN on the three datasets CIFAR-10, MNIST and FMNIST by 2.44%, 1.77%, and 1.73%, respectively.

## II. RELATED WORK

We briefly review the related works in term of one-class novelty detection and knowledge distillation.

### A. One-class Novelty Detection

In the semi-supervised one-class novelty detection, only the normal samples with one class are used for training the model. Conventionally, novelty detection methods can be

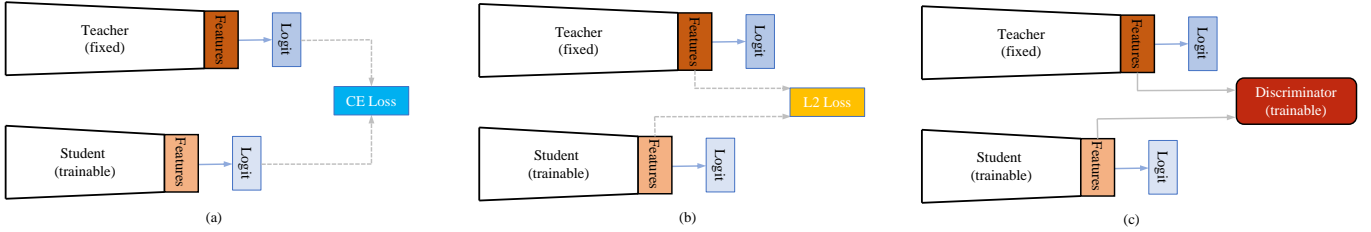


Fig. 2: Comparison with different knowledge distillation architectures.

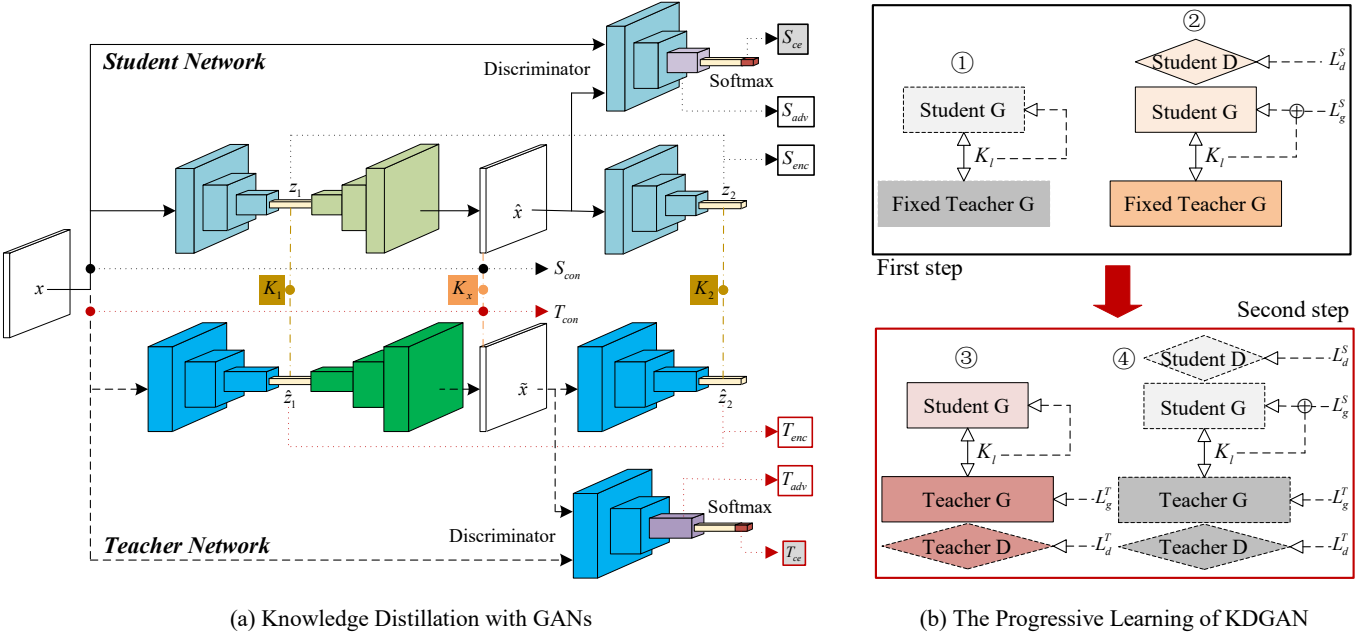


Fig. 3: The flowchart of Knowledge Distillation with GANs for One-class Novelty Detection. (a) The Knowledge Distillation with Generative Adversarial Networks (KDGAN), in which the distillation losses  $K_l$  ( $K_l = w_1 K_1 + w_x K_x + w_2 K_2$ ) is designed for training the student GAN. (b) The two-step progressive learning of KDGAN is used to continuously improve the performance of the student GAN, in which P-KDGAN-②④ achieves the best performance. KDGAN-①, KDGAN-②, KDGAN-③ and KDGAN-④ are four different distillation structures.

divided into two categories [6]. One is the traditional methods, such as One-Class SVM (OC-SVM) [45], Kernel Density Estimation (KDE) [32] and Principal Component Analysis (PCA) [53]. The disadvantage of such approaches is that they are not suitable for high-dimensional image data. The other methods based on deep learning include Deep Belief Networks (DBN) [10], Autoencoders (AE) [49] and generative adversarial networks (GANs) [44], [57], [36].

GANs have shown state-of-the-art performance in modeling complex high-dimensional image distributions [14]. Therefore, a lot of GANs based methods have been used for novelty detection [44], [57], [36]. The reconstruction error between inputs and reconstructed images or two latent vectors are utilized as the novelty score, which means that the learned model only reconstructs normal samples well, and shows very low tolerance for novel samples. Schlegl et al. [44] proposed the first GAN-based work, AnoGAN, for novelty detection. In training, the combination of the residual loss on images and the discrimination loss on feature maps is minimized to iteratively search the best latent vector. The Efficient GAN [57] based on

BiGAN [9] network was proposed for jointly training the map from the image to the latent space simultaneously. Perera et al. [36] proposed the OCGAN in which two discriminators were used in the latent space and the input space for making the learned network better model the input images. Recently, Ganomaly [2] constructs a novel architecture EDE-GAN using the residual loss in latent space as anomaly score for “MISO” task. Skip-Ganomaly used the skip connections to thoroughly capture the multi-scale distribution of the normal data distribution in high-dimensional image space.

### B. Knowledge Distillation

To reduce the large computation and storage cost of deep convolutional neural networks, knowledge distillation can transfer the generalization ability of a large network (or an ensemble of networks) to a light-weight network. Figure 2 (a), Hinton et al. [15] used the outputs of the softmax layer of a teacher network as the target function to train the student network. Romero et al. [39], illustrated in Figure 2

(b), proposed that a student network with random initialization can imitate the intermediate representations of the teacher network to improve its own performance. In order to ensure the student network to learn the true data distribution from the teacher network, knowledge distillation with a discriminator was used for distinguishing features extracted from the teacher and student networks, Figure 2 (c) [51], [52], [25]. Li et al. [24] combined neural architecture search and knowledge distillation to compress the generator for controllable image synthesis.

GANs [14] have been applied to many real world applications such as domain adaptation, image generation, and anomaly detection. However, to our knowledge, there is no related works that deploy the knowledge distillation on two standard GANs. Therefore, this paper designs a distillation loss to transfer knowledge from the teacher GAN to the student GAN, in which knowledge distillation is considered as a progressive learning process that can continuously improve the performance of student networks.

### III. METHOD

In this section, we firstly analyze the impacts of the batch size on one-class novelty detection, and then introduce three different network architectures that will be used to perform comparative experiments to illustrate the superiority of EDE-GAN. Afterwards, the distillation loss based on the EDE-GAN model and four different distillation structures are proposed to transfer knowledge. Finally, we propose a two-step Progressive Knowledge Distillation with GANs (P-KDGAN) to learn a light-weight student GAN from a pre-trained teacher GAN.

#### A. Analysis on Batch Size

The evaluation metric, Area Under Curve (AUC), can be written as:

$$AUC = \frac{\sum_{i \in Normal} R_i - \frac{N \times (N+1)}{2}}{M \times N} \quad (1)$$

where  $R$  denotes the index of sorted prediction probabilities, and  $M, N$  represent the number of samples on the normal and abnormal classes.

Based on the Eq. 1, in order to improve the generalization of model, we need to reduce the over-fitting on normal training data, *i.e.* reduce their prediction confidences to increase the sum of the index values of normal samples  $\sum_{i \in Normal} R_i$ . As we know, for different batch sizes, there are trade-offs between fitting and generalization. When the batch size equals to 1, as illustrated in Figure 1 and Figure 5, the models can achieve the best performances. The above results demonstrate that the models can well learn the identity of each normal sample, at the same time, large gradient noise and the constraint on the latent space avoid the over-fitting. However, when the batch size is larger than 1, we can think that the fitting ability of the model is greatly weakened. Because the BN needs to model features of different samples on the channels, *i.e.*, a single sample will be severely affected by the same min-batch samples, resulting in poor testing performance and difficulty in optimization [55].

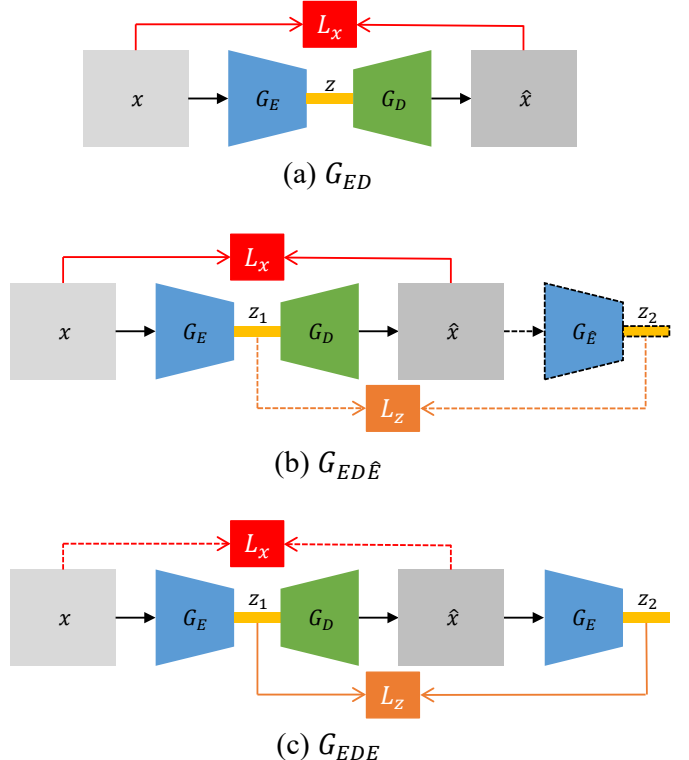


Fig. 4: Comparison with different generator architectures for novelty detection, in which the discriminators are not used during inference. The “dotted” lines indicate that the modules and losses are only used during the training. (a)  $G_{ED}$  based on encoder-decoder pipeline uses the reconstruction error  $L_x$  between images as the anomaly score. (b)  $G_{ED\hat{E}}$  is used for training where  $G_{\hat{E}}$  and  $L_z$  do not participate in the inference progress.  $L_z$  is the reconstruction error between two latent vectors  $z_1$  and  $z_2$ . (c)  $G_{EDE}$  based on encoder-decoder-encoder scheme uses the  $L_z$  as the anomaly score.

#### B. Three GAN Architectures

GAN-based novelty detection emerges quickly as one of the popular detection approaches after its early use in [44]. GAN consists of two adversarial modules, a generator  $G$  that learns the distribution of the input image  $x$  from the latent spaces, and a discriminator  $D$  that decides whether the reconstructed image  $\hat{x}$  is real or fake.  $D$  and  $G$  are simultaneously optimized by playing the following minmax game as:

$$\min_G \max_D V(D, G) = \mathbb{E}_{x \sim \mathbf{X}}[\log D(x)] + \mathbb{E}_{x \sim \mathbf{X}}[\log(1 - G(x))], \quad (2)$$

where training dataset  $\mathbf{X}$  comprises  $N$  normal images,  $\mathbf{X} = [\mathbf{x}_1, \mathbf{x}_2, \dots, \mathbf{x}_N] \in \mathbb{R}^{N \times w \times h \times c}$ , and  $\mathbb{E}_{x \sim \mathbf{X}}$  is the expected value of  $x$  obeying the distribution of normal images  $\mathbf{X}$ .

Figure 4 shows three different generator networks for novelty detection, in which the discriminators are not illustrated. The differences between the above three architectures include the following two points: one is the definition of anomaly score, and the other is the loss function that constrains the latent space.

Symbol	Equation	Explanation
<b><i>GAN Loss</i></b>		
$L_g^S, L_g^T$	$L_g^S = w_{con}S_{con} + w_{enc}S_{enc} + w_{adv}S_{adv}$	Generator loss
$L_d^S, L_d^T$	$L_d^S = S_{ce}$	Discriminator loss
$S_{con}, T_{con}$	$S_{con} = \mathbb{E}_{\mathbf{x} \sim \mathbf{X}} \ \mathbf{x} - \hat{\mathbf{x}}\ _1$	Reconstruction errors of images
$S_{enc}, T_{enc}$	$S_{enc} = \mathbb{E}_{\mathbf{x} \sim \mathbf{X}} \ \mathbf{z}_1 - \mathbf{z}_2\ _2$	Reconstruction errors of latent vectors
$S_{adv}, T_{adv}$	$S_{adv} = \mathbb{E}_{\mathbf{x} \sim \mathbf{X}} \ f(\mathbf{x}) - f(\hat{\mathbf{x}})\ _2$	Discriminator losses on feature maps
$S_{ce}, T_{ce}$	$S_{ce} = -[\mathbf{y} \log \hat{\mathbf{y}} + (1 - \mathbf{y}) \log(1 - \hat{\mathbf{y}})]$	Discriminator CE loss
<b><i>Distillation Loss</i></b>		
$K_l$	$K_l = w_1K_1 + w_xK_x + w_2K_2$	Distillation loss
$K_1$	$K_1 = \ \mathbf{z}_1 - \hat{\mathbf{z}}_1\ _2$	Distance between former latent vectors
$K_x$	$K_x = \ \hat{\mathbf{x}} - \tilde{\mathbf{x}}\ _1$	Distance between reconstructed images
$K_2$	$K_2 = \ \mathbf{z}_2 - \hat{\mathbf{z}}_2\ _2$	Distance between later latent vectors

TABLE I: The symbols and their corresponding equations and explanations in this paper.

- $G_{ED}$  shown in Figure 4 (a) uses the reconstruction error  $L_x$  ( $L_x = \|\mathbf{x} - \hat{\mathbf{x}}\|_1$ ) between input image  $x$  and reconstructed image  $\hat{\mathbf{x}}$  as the anomaly score for detection, and there is no constraint on the latent space.
- $G_{EDE}$  based on the encoder-decoder-encoder pipeline, illustrated in Figure 4 (c), uses the residual loss  $L_z$  ( $L_z = \|\mathbf{z} - \hat{\mathbf{z}}\|_2$ ) as the anomaly score, and the constraint  $L_z$  is used for training.
- In order to demonstrate the superiority of  $G_{EDE}$  and the effectiveness of the constraint on the latent space, we design a new GAN architecture  $G_{ED\hat{E}}$  (Figure 4 (b)), in which the second encoder  $G_{\hat{E}}$  and constraint loss  $L_z$  are only used during training, hence  $L_z$  is the novelty score.

### C. KDGAN

In the KDGAN, we design a distillation loss based on EDE-GAN to solve problem (1) described in Section I. As shown in Figure 3, the difference between them is the number of channels in each layer. The generator loss  $L_g^S$  of the student GAN includes reconstructed image loss  $S_{con}$ , latent space loss  $S_{enc}$  and adversarial loss  $S_{adv}$ :

$$S_{con} = \mathbb{E}_{\mathbf{x} \sim \mathbf{X}} \|\mathbf{x} - \hat{\mathbf{x}}\|_1, \quad (3)$$

$$S_{enc} = \mathbb{E}_{\mathbf{x} \sim \mathbf{X}} \|\mathbf{z}_1 - \mathbf{z}_2\|_2, \quad (4)$$

$$S_{adv} = \mathbb{E}_{\mathbf{x} \sim \mathbf{X}} \|f(\mathbf{x}) - f(\hat{\mathbf{x}})\|_2, \quad (5)$$

$$L_g^S = w_{con}S_{con} + w_{enc}S_{enc} + w_{adv}S_{adv}, \quad (6)$$

where  $f(\cdot)$  outputs the intermediate representations of discriminator  $D$ .  $S_{con}$ ,  $S_{enc}$  and  $S_{adv}$  denote the reconstruction errors of the images, latent vectors and feature maps, respectively. The weighted sum of  $S_{con}$ ,  $S_{enc}$  and  $S_{adv}$  constitutes the

generator loss  $L_g^S$  and is minimized to train the student generator  $G$ .

The designed distillation loss  $K_l$  is a novel attempt for knowledge distillation on two standard GANs. As shown in Figure 3 (a), the teacher GAN and the student GAN transfer knowledge through the intermediate layers of the generators, which includes two latent vectors and one reconstructed images. In the KDGAN, we design three losses  $K_1$ ,  $K_x$  and  $K_2$  to measure the similarity of the intermediate layers.  $K_1$  and  $K_2$  are the  $L_2$  distance of latent vectors ( $\mathbf{z}_1$  and  $\hat{\mathbf{z}}_1$ ,  $\mathbf{x}_2$  and  $\hat{\mathbf{x}}_2$ ) from the teacher GAN and student GAN.  $K_x$  is the  $L_1$  distance of reconstructed images ( $\hat{\mathbf{x}}$ ,  $\tilde{\mathbf{x}}$ ). Based on the above three losses, we propose distillation loss  $K_l$  as an objective function for knowledge distillation which is the weighted sum of  $K_1$ ,  $K_x$  and  $K_2$ :

$$K_l = w_1K_1 + w_xK_x + w_2K_2, \quad (7)$$

$$K_1 = \|\mathbf{z}_1 - \hat{\mathbf{z}}_1\|_2, \quad (8)$$

$$K_x = \|\hat{\mathbf{x}} - \tilde{\mathbf{x}}\|_1, \quad (8)$$

$$K_2 = \|\mathbf{z}_2 - \hat{\mathbf{z}}_2\|_2. \quad (8)$$

We summarize the symbols and their corresponding equations in Table I.

### D. Four Distillation Structures

As is illustrated in Figure 3 (a), the designed distillation loss  $K_l$  builds a “bridge” between the teacher and student GANs for knowledge transfer. The losses in the KDGAN consist of three parts: teacher GAN losses  $L_g^T, L_d^T$ , student GAN losses  $L_g^S, L_d^S$ , and distillation loss  $K_l$ . We define the above five loss functions as the elements of set  $\mathcal{L}$ :

$$\mathcal{L} = \{\alpha L_g^T, \beta L_d^T, \mu L_g^S, \nu L_d^S, \lambda K_l\}, \quad (9)$$

where  $\alpha, \beta, \mu, \nu$ , and  $\lambda \in \{0, 1\}$  indicates whether the corresponding loss is used to train the networks.

**Algorithm 1** Progressive Knowledge Distillation with GANs

**Input:** Pre-trained teacher  $G$  and  $D$ , training dataset with normal instances  $(x_i, y_i)_{i=1}^N$ , epoch  $T$

**Output:** Improved student  $G$

```

1: First step
2: Student  $G$  and  $D$  with random initialization
3: for  $t=1$  to  $T$  do
4:   for  $i=1$  to  $N$  do
5:     Update student  $G$  and  $D$  when teacher GAN with
       fixed weights
6:   end for
7: end for
8: Second step
9: Download the weights of the teacher and student GANs
   from the previous last epoch
10: for  $t=1$  to  $T$  do
11:   for  $i=1$  to  $N$  do
12:     Update teacher  $G$  and  $D$ 
13:     Update student  $G$  and  $D$ 
14:   end for
15: end for

```

The elements in  $\mathcal{L}$  can be combined into four subsets ( $\mathcal{L}_1$ ,  $\mathcal{L}_2$ ,  $\mathcal{L}_3$ ,  $\mathcal{L}_4$ ) to form different distillation structures according to the following two rules. The first rule is whether the teacher GAN has fixed weights; the second rule is whether the distillation loss  $K_l$  is combined with the losses  $L_g^S$ ,  $L_d^S$  to train the student GAN. Before the KDGAN, a teacher GAN is trained by its own generator loss  $L_g^T$  and discriminator loss  $L_d^T$ . The designed four distillation structures are introduced as follows.

- **KDGAN-①:**  $\mathcal{L}_1=\{K_l\}$ . Without the use of real labels, the training of the student network only depends on the distillation loss  $K_l$ , which results in poor detection performance. There is no adversarial networks, and the teacher network is not updated, so its training speed is the fastest.
- **KDGAN-②:**  $\mathcal{L}_2=\{L_g^S, L_d^S, K_l\}$ . The student GAN is trained by minimizing its own losses  $L_g^S$ ,  $L_d^S$  and distillation loss  $K_l$ , while the teacher GAN is not updated. The adversarial network in student GAN causes its training speed to be slightly slower than KDGAN-①.
- **KDGAN-③:**  $\mathcal{L}_3=\{L_g^T, L_d^T, K_l\}$ . The teacher GAN uses its own losses  $L_g^T$ ,  $L_d^T$  to train to maintain its performance, when the training of the student GAN follows KDGAN-①. Its training speed is almost the same as that of KDGAN-②.
- **KDGAN-④:**  $\mathcal{L}_4=\{L_g^T, L_d^T, L_g^S, L_d^S, K_l\}$ . The trainings of the teacher and student GANs follow KDGAN-③ and KDGAN-②, respectively. There are two adversarial networks that need to be trained simultaneously, so the training speed is the lowest.

*E. Progressive Learning of KDGAN*

The progressive learning of KDGAN, shown in Figure 3 (b), is a two-step approach that continuously improves

the performance of the student GAN and achieves better performance than those single step methods. The two-step P-KDGAN is described as follows.

*a) P-KDGAN-I.*: In the first step, four distillation structures are utilized to train the student network. The experimental results shown in Section IV-E demonstrate that the performance of the student network with random initialization has a large gap compared with the teacher network. Therefore, considering the detection accuracy and training time of the four distillation structures, KDGAN-② is used as the first step of P-KDGAN to enable the student network to learn the basics knowledge from the teacher network. In KDGAN-②, the pre-trained teacher has already converged, so the teacher network with fixed weights is used to train the student network relying on real labels and distillation knowledge. Such a “teaching by teacher” step makes the student learn the basic knowledge totally from the teacher.

*b) P-KDGAN-II.*: In the second step, KDGAN-③ and KDGAN-④ continue to train the teacher networks, while the student networks with basic knowledge rely on distilling knowledge to fine-training, thereby further improving accuracy and stability. The fine-learning processes in this step are named as P-KDGAN-II-②③ and P-KDGAN-II-②④. The experimental results prove that the performance of the student network even exceeds the teacher network in some categories of one-class novelty detection.

The above process is illustrated in Algorithm 1.

**IV. EXPERIMENTS**

In this section, the proposed P-KDGAN is evaluated on the well-known CIFAR-10 [20], MNIST [21] and FMNIST [56] datasets. Following previous work [36], we quantify the performance of our method using the Area Under Curve (AUC) of Receiver Operating Characteristics (ROC). The detailed analysis on the results and comparative experiments with state of the art techniques are introduced as follows.

All the reported results are implemented using the PyTorch framework [33] on NVIDIA RTX 2080TI. In our experiments, the batch size and epoch are set to 1 and 500 respectively. We apply Adam [18] with  $\beta_1 = 0.5$  and  $\beta_2 = 0.99$  to optimize model parameters with a learning rate of 0.002.

*A. Datasets*

For the three experimental datasets, the training and testing partitions remain as default. In the setup, one of the classes from training dataset is considered as normal samples for training. During testing, the remaining classes are used to represent novelty samples. For example, every experiment on the CIFAR-10 dataset is trained with 5000 samples and tested with 10,000 samples. The above experiments are repeated for all ten categories. In addition, in order to be compatible with the network architectures, all images are resized to  $32 \times 32$  by Bilinear interpolation.

*• CIFAR-10:* consists of 60,000  $32 \times 32$  RGB images in 10 classes, with 6,000 images for per class. Each category contains 50,00 training images and 10,000 test images.

Layer	Teacher-Units	Student-Units	BN	Activation	Kernel
<i>E(x)</i>					
Conv2D	64	$u$	✓	LeakyReLU	$4 \times 4$
Conv2D	128	$2 \times u$	✓	LeakyReLU	$4 \times 4$
Conv2D	256	$4 \times u$	✓	LeakyReLU	$4 \times 4$
Conv2D	256	256			$4 \times 4$
<i>D(x)</i>					
ConvTrans2D	256	$4 \times u$	✓	ReLU	$4 \times 4$
ConvTrans2D	128	$2 \times u$	✓	ReLU	$4 \times 4$
ConvTrans2D	64	$u$	✓	ReLU	$4 \times 4$
ConvTrans2D	3	3		Tanh	$4 \times 4$

TABLE II: The encoder and decoder architectures for our teacher GAN and student GAN, layer by layer. Units refer to number of filters in the case of convolution layers, and BN is Batch Normalization abbreviated.  $u$  represents the number of channels in the layer, and it has different value on every dataset, that is, student network with different size of parameters.

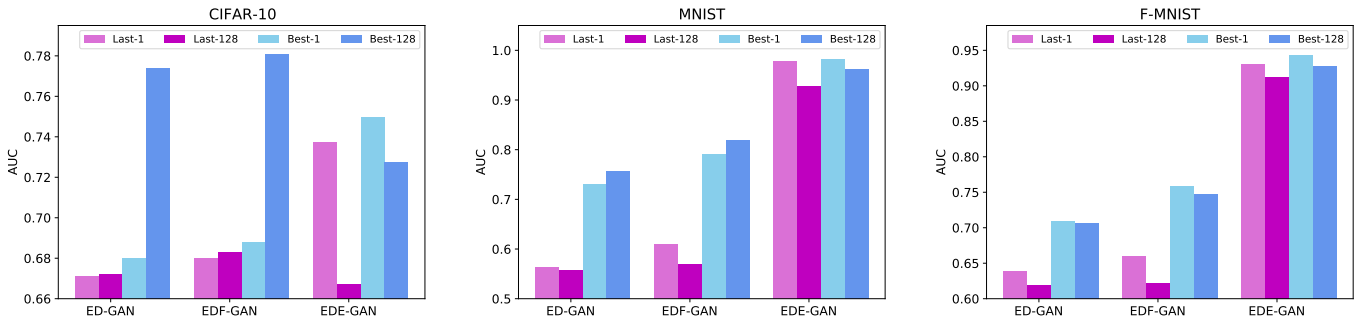


Fig. 5: Compare the Last / Best performance of ED-GAN, EDF-GAN and EDE-GAN based on different batch size. EDF-GAN represents ED $\hat{E}$ -GAN.

Hyper-parameter	Value
$w_{con}$	10
$w_{enc}$	1
$w_{adv}$	1
$w_1$	1
$w_x$	1
$w_2$	1

TABLE III: The hyper-parameters in our experiments.

- **MNIST:** consists of 70,000  $28 \times 28$  hand-written grayscale digit images from 0-9. The training set has 60,000 images and the test set has 10,000 images.
- **FMNIST:** similars to MNIST, in which the images are from an online clothing store. The  $28 \times 28$  grayscale images of 70,000 fashion products from 10 categories, with 7,000 images per category. The number of training and testing images are as same as MNIST.

### B. Network Architectures

The encoder  $E(x)$  and decoder  $D(x)$  in ED-GAN, ED $\hat{E}$ -GAN and EDE-GAN frameworks follow the DCGAN [38] architecture, which have three basic layers in our model. As shown in Table II, the basic layers consist of convolutional layers (deconvolutional layers), batch normalization and activation. In contrast, LeakyReLU and ReLU activations are used in encoders and decoders, except for the last layer in decoder, which uses Tanh. All the convolution filters are set to  $4 \times 4$ .

In the following P-KDGAN experiments, the difference between a teacher network and a student network is the number of channels in the intermediate representations. For the three experimental datasets, the intermediate layers in the teacher networks are set to 64-128-256 channels following the OCGAN [36]. The student networks in each dataset utilize intermediate representations with 8-16-64 channels, 2-4-8 channels and 1-2-4 channels respectively ( $u = 8, 2, 1$  respectively). The encoder  $E(x)$  and decoder  $D(x)$  architecture of the teacher GAN is illustrated in Table II.

### C. Comparison with EDE-GAN

As shown in Figure 5, the EDE-GAN model achieves the best results in the “Last” performance on three datasets,

NORMAL CLASS	OCSVM	KDE	VAE	AND	AnoGAN	DSVDD	OCGAN	Ours
AIRPLANE	0.630	0.658	0.700	0.717	0.671	0.617	0.757	<b>0.825</b>
AUTOMOBILE	0.440	0.520	0.386	0.494	0.547	0.659	0.531	<b>0.744</b>
BIRD	0.649	0.657	0.679	0.662	0.529	0.508	0.640	<b>0.703</b>
CAT	0.487	0.497	0.535	0.527	0.545	0.591	<b>0.620</b>	0.605
DEER	0.735	0.727	0.748	0.736	0.651	0.609	0.723	<b>0.765</b>
DOG	0.500	0.496	0.523	0.504	0.603	<b>0.657</b>	0.620	0.652
FROG	0.725	0.758	0.687	0.726	0.585	0.677	0.723	<b>0.797</b>
HORSE	0.533	0.564	0.493	0.560	0.625	0.673	0.575	<b>0.723</b>
SHIP	0.649	0.680	0.696	0.680	0.758	0.759	0.820	<b>0.827</b>
TRUCK	0.508	0.540	0.386	0.566	0.665	0.731	0.554	<b>0.735</b>
MEAN	0.5856	0.6097	0.5833	0.6172	0.6179	0.6481	0.6566	<b>0.7376</b>
0	0.988	0.885	0.997	0.984	0.966	0.980	<b>0.998</b>	0.996
1	0.999	0.996	0.999	0.995	0.992	0.997	<b>0.999</b>	<b>0.999</b>
2	0.902	0.710	0.936	0.947	0.850	0.917	0.942	<b>0.969</b>
3	0.950	0.693	0.959	0.952	0.887	0.919	0.963	<b>0.969</b>
4	0.955	0.844	0.973	0.960	0.894	0.949	<b>0.975</b>	0.970
5	0.968	0.776	0.964	0.971	0.883	0.885	<b>0.980</b>	0.951
6	0.978	0.861	0.993	0.991	0.947	0.983	0.991	<b>0.992</b>
7	0.965	0.884	0.976	0.970	0.935	0.946	0.981	<b>0.982</b>
8	0.853	0.669	0.923	0.922	0.849	0.939	0.939	<b>0.965</b>
9	0.955	0.825	0.976	0.979	0.924	0.965	0.981	<b>0.987</b>
MEAN	0.9513	0.8143	0.9696	0.9671	0.9127	0.9480	0.9750	<b>0.9780</b>

TABLE IV: One-class novelty detection results on CIFAR-10 and MNIST datasets. The average AUC of three repeated experiments was used as the detection performance.

Dataset	Method	AUC. $\downarrow$	#Param. $\downarrow$	#FLOPs. $\downarrow$
CIFAR-10	Teacher	73.76%	5.12M	56M
	Student	3.15%		
	P-KDGAN	<b>0.71%</b>	6.22 $\times$	24.45 $\times$
MNIST	Teacher	97.80%	5.12M	56M
	Student	2.32%		
	P-KDGAN	<b>0.55%</b>	52.22 $\times$	311.11 $\times$
FMNIST	Teacher	93.11%	5.12M	56M
	Student	1.91%		
	P-KDGAN	<b>0.18%</b>	105.45 $\times$	700 $\times$

TABLE V: Evaluation of our P-KDGAN method on CIFAR-10, MNIST and FMNIST datasets. (M means million, # means the compression ratio of parameter numbers and FLOPs compared to the teacher GAN.)

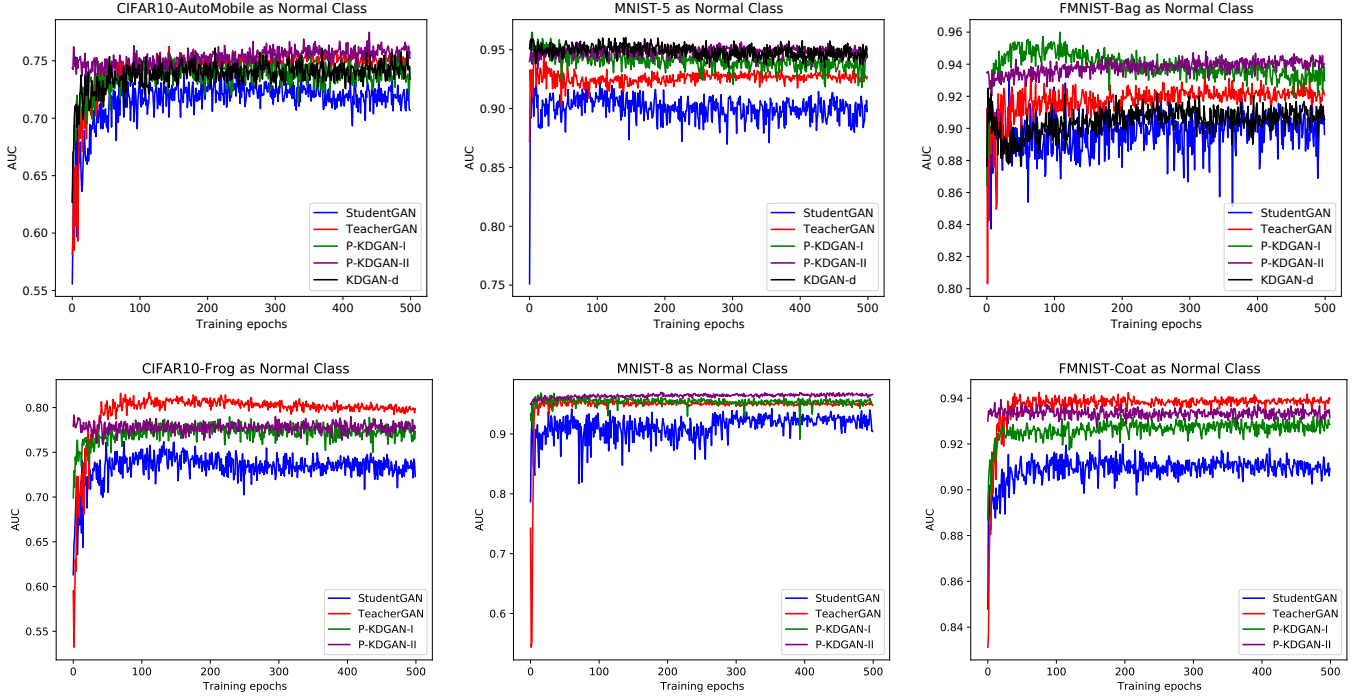


Fig. 6: Training curves of the AUC on three datasets. The normal classes are: (a) AutoMobile on CIFAR-10. (b) 5 on MNIST. (c) Bag on FMNIST. P-KDGAN-I represents KDGAN-②. P-KDGAN-II represents P-KDGAN-II-②③. KDGAN-d represents KDGAN-④.

Method	CIFAR-10	MNIST	FMNIST
KDGAN-①	71.59%	96.7%	92.48%
KDGAN-②	72.43%	96.75%	92.41%
KDGAN-③	70.94%	97.18%	92.90%
KDGAN-④	72.58%	96.87%	92.42%
P-KDGAN-II-②③	73.05%	97.25%	92.93%
P-KDGAN-II-②④	72.52%	96.67%	92.57%

TABLE VI: Compare the performance of KDGAN and P-KDGAN. We highlight the best results in red color and the second-best results in blue color.

and exceeds the runner-up by 5.74%, 36.92% and 27.15% respectively excepting for the “BEST” performance on the CIFAR-10 data. Compared with ED-GAN, the new designed ED-GAN improves the “LAST” performance by 0.91%, 4.66% and 2.08% on three datasets respectively by using the constraint on the latent vectors for training when  $B = 1$ . The above experimental results illustrate the beneficial constraint on the latent space, and the novelty score on latent vectors is more robust to noise.

#### D. Results on One-class Novelty Detection

In this section, we compare our Gandomaly [2] based Teacher GAN with several traditional and deep learning based methods

on CIFAR-10 and MNIST datasets, including one-class SVM (OC-SVM) [45], kernel density estimation (KDE) [32], deep variational autoencoder (VAE) [19], AND [1], AnoGAN [44], DSVDD [40] and OCGAN [36]. In light of massive experiments, the parameters of  $w_{con}$ ,  $w_{enc}$  and  $w_{adv}$  in Eq. 6 are manually configured as 10, 1 and 1. The parameters of  $w_1$ ,  $w_x$  and  $w_2$  in Eq. 7 are set as 1. We take the average AUC of the last epoch from multiple trials, but not the manually selected result, as the detection performance, which is more convicitive.

**Comparisons on CIFAR-10 and MNIST.** For one-class novelty detection on CIFAR-10 dataset, our method achieves the result of 73.76% as shown in Table IV, which is higher than the best OCGAN [36] method about 8%. For MNIST dataset, our method achieves 97.80% yielding an improvement of about 0.3% compared with the state-of-the-art method.

#### E. Evaluation of P-KDGAN Method

In this section, the progressive knowledge distillation with GANs is evaluated on CIFAR-10, MNIST and FMNIST datasets. What we would like to highlight that the model weights of of last epoch are served as the teacher network in our experiment.

**KDGAN vs. P-KDGAN.** As is shown in Table VI, P-KDGAN-II-②③ achieves the best performance on three datasets, which illustrates the effectiveness of our progressive learning of KDGAN. Although KDGAN-③ achieves the second-best results on MNIST and FMNIST, it shows the worst performance on CIFAR-10 dataset. KDGAN-④ obtains

the second-best results on CIFAR-10, but it is about 0.5% lower than the best result. In addition, KDGAN-d (KDGAN-④) illustrated in Figure 6(c) is inferior in accuracy and training stability compared to P-KDGAN-II. The training curves of the AUC illustrated in Figure 6 clearly show that proposed P-KDGAN-II can improve the accuracy of the student network and even surpass the teacher network, and reduce shock. Therefore, the above analysis concludes that student networks with random initialization can only learn the basic knowledge of the teacher networks, and the fine-training in the second step of P-KDGAN can further improve performance.

**Results on P-KDGAN.** As illustrated in Table V, the performance of the student GAN obtained by two-step P-KDGAN is only 0.71%, 0.55% and 0.18% lower than that of the teacher GAN when compressing the computation at ratios of 24.45:1, 311.11:1, and 700:1, respectively.

## V. CONCLUSION AND DISCUSSION

In this paper, we use the EDE-GAN for one-class novelty detection and achieve state-of-the-art performance. We firstly design a new GAN architecture and perform comparative experiments to demonstrate the beneficial constraint on the latent space. To compress the model, the progressive knowledge distillation with GANs is proposed, which is a novel exploration that applies the knowledge distillation on two standard GANs. The two-step progressive learning can continuously improve the performance and reduce shock of the student network, in which the designed distillation loss plays an important role. Experiments on three datasets validate the effectiveness of our proposed method.

We hope the proposed method will open new avenues of solution for one-class novelty detection and other related problems, and make the following summary:

1) Re-evaluate the performance of all other methods on the one-class novelty detection task based on different batch sizes, and we need to consider the performance of model in the last epoch, rather than selecting the best result in all epochs for display.

2) We are looking forward to the application of our proposed P-KDGAN on other tasks, such as image dehazing, image super-resolution and image synthesis.

3) Since novelty detection is different from traditional classification problem, we may need to rethink how Batch Normalization can be improved on this task.

## VI. ACKNOWLEDGMENT

This work is supported by Key-Area Research and Development Program of Guangdong Province (2019B010155003), Shenzhen Science and Technology Innovation Commission (JCYJ20200109114835623), and National Natural Science Foundation of China (U1713203).

## REFERENCES

- [1] Davide Abati, Angelo Porrello, Simone Calderara, and R. Cucchiara. Latent space autoregression for novelty detection. *2019 IEEE/CVF Conference on Computer Vision and Pattern Recognition (CVPR)*, pages 481–490, 2019.
- [2] Samet Akcay, Amir Atapour-Abarghouei, and Toby P Breckon. Ganomaly: Semi-supervised anomaly detection via adversarial training. In *Asian conference on computer vision*, pages 622–637. Springer, 2018.
- [3] S. Akçay, Amir Atapour-Abarghouei, and T. Breckon. Skip-ganomaly: Skip connected and adversarially trained encoder-decoder anomaly detection. In *2019 International Joint Conference on Neural Networks (IJCNN)*, pages 1–8, 2019.
- [4] Philippe Burlina, Neil Joshi, and I-Jeng Wang. Where’s wally now? deep generative and discriminative embeddings for novelty detection. *CVPR*, pages 11499–11508, 2019.
- [5] Raghavendra Chalapathy, Aditya Krishna Menon, and Sanjay Chawla. Anomaly detection using one-class neural networks. *arXiv preprint arXiv:1802.06360*, 2018.
- [6] Varun Chandola, Arindam Banerjee, and Vipin Kumar. Anomaly detection : A survey. *ACM Comput. Surv.*, 41(3):1–72, 2009.
- [7] Jiacheng Cheng and Nuno Vasconcelos. Learning deep classifiers consistent with fine-grained novelty detection. In *Proceedings of the IEEE/CVF Conference on Computer Vision and Pattern Recognition*, pages 1664–1673, 2021.
- [8] Y. Cheng, D. Wang, P. Zhou, and T. Zhang. A survey of model compression and acceleration for deep neural networks. *ArXiv*, abs/1710.09282, 2017.
- [9] Jeff Donahue, Philipp Krähenbühl, and Trevor Darrell. Adversarial feature learning. *ICLR*, 2017.
- [10] Sarah M. Erfani, Sutharshan Rajasegarar, Shanika Karunasekera, and Christopher Leckie. High-dimensional and large-scale anomaly detection using a linear one-class svm with deep learning. *Pattern Recognition*, 58:121–134, 2016.
- [11] Pedro García-Teodoro, Jesús E. Díaz-Verdejo, Gabriel Maciá-Fernández, and Enrique Vázquez. Anomaly-based network intrusion detection: Techniques, systems and challenges. *Comput. Secur.*, 28(1-2):18–28, 2009.
- [12] Izhak Golani and Ran El-Yaniv. Deep anomaly detection using geometric transformations. In *Advances in Neural Information Processing Systems*, volume 31, pages 9758–9769, 2018.
- [13] Dong Gong, L. Liu, Vuong Le, Budhaditya Saha, M. Mansour, S. Venkatesh, and A. V. D. Hengel. Memorizing normality to detect anomaly: Memory-augmented deep autoencoder for unsupervised anomaly detection. *2019 IEEE/CVF International Conference on Computer Vision (ICCV)*, pages 1705–1714, 2019.
- [14] Ian J. Goodfellow, Jean Pouget-Abadie, Mehdi Mirza, Bing Xu, David Warde-Farley, Sherjil Ozair, Aaron C. Courville, and Yoshua Bengio. Generative adversarial nets. *NeurIPS*, 2014.
- [15] Geoffrey E. Hinton, Oriol Vinyals, and Jeffrey Dean. Distilling the knowledge in a neural network. *ArXiv*, abs/1503.02531, 2015.
- [16] Sergey Ioffe and Christian Szegedy. Batch normalization: Accelerating deep network training by reducing internal covariate shift. In *International conference on machine learning*, pages 448–456. PMLR, 2015.
- [17] Eric Jardim, Lucas A Thomaz, Eduardo AB da Silva, and Sergio L Netto. Domain-transformable sparse representation for anomaly detection in moving-camera videos. *IEEE Transactions on Image Processing*, 29:1329–1343, 2019.
- [18] Diederik P. Kingma and Jimmy Ba. Adam: A method for stochastic optimization. *CoRR*, abs/1412.6980, 2015.
- [19] Diederik P. Kingma and Max Welling. Auto-encoding variational bayes. *CoRR*, abs/1312.6114, 2014.
- [20] Alex Krizhevsky. Learning multiple layers of features from tiny images. 2009.
- [21] Yann LeCun and Corinna Cortes. The mnist database of handwritten digits. 2005.
- [22] Roberto Leyva, Victor Sanchez, and Chang-Tsun Li. Video anomaly detection with compact feature sets for online performance. *IEEE Transactions on Image Processing*, 26(7):3463–3478, 2017.
- [23] Chun-Liang Li, Kihyuk Sohn, Jinsung Yoon, and Tomas Pfister. Cut-paste: Self-supervised learning for anomaly detection and localization. In *Proceedings of the IEEE/CVF Conference on Computer Vision and Pattern Recognition*, pages 9664–9674, 2021.
- [24] Muyang Li, Ji Lin, Yaoyao Ding, Zhijian Liu, Jun-Yan Zhu, and Song Han. Gan compression: Efficient architectures for interactive conditional gans. In *Proceedings of the IEEE/CVF Conference on Computer Vision and Pattern Recognition*, pages 5284–5294, 2020.
- [25] Peiye Liu, Wu Liu, Huadong Ma, Tao Mei, and Mingoo Seok. Ktan: knowledge transfer adversarial network. *ArXiv*, abs/1810.08126, 2018.
- [26] Weining Lu, Yu Cheng, Cao Xiao, Shiyu Chang, Shuai Huang, Bin Liang, and Thomas Huang. Unsupervised sequential outlier detection with deep architectures. *IEEE transactions on image processing*, 26(9):4321–4330, 2017.

[27] Cuong Phuc Ngo, Amadeus Aristo Winarto, Connie Khor Li Kou, Sojeong Park, Farhan Akram, and Hwee Kuan Lee. Fence gan: Towards better anomaly detection. In *2019 IEEE 31st International Conference on Tools with Artificial Intelligence (ICTAI)*, pages 141–148, 2019.

[28] Guansong Pang, Chunhua Shen, Longbing Cao, and Anton van den Hengel. Deep learning for anomaly detection: A review. *arXiv preprint arXiv:2007.02500*, 2020.

[29] Guansong Pang, Chunhua Shen, Huidong Jin, and Anton van den Hengel. Deep weakly-supervised anomaly detection. *arXiv*, pages arXiv-1910, 2019.

[30] Guansong Pang, Chunhua Shen, and Anton van den Hengel. Deep anomaly detection with deviation networks. In *Proceedings of the 25th ACM SIGKDD International Conference on Knowledge Discovery & Data Mining*, pages 353–362, 2019.

[31] Guansong Pang, Cheng Yan, Chunhua Shen, Anton van den Hengel, and Xiao Bai. Self-trained deep ordinal regression for end-to-end video anomaly detection. In *Proceedings of the IEEE/CVF Conference on Computer Vision and Pattern Recognition*, pages 12173–12182, 2020.

[32] Emanuel Parzen. On estimation of a probability density function and mode. *Annals of Mathematical Statistics*, 33(3):1065–1076, 1962.

[33] Adam Paszke, Sam Gross, Soumith Chintala, Gregory Chanan, Edward Yang, Zachary Devito, Zeming Lin, Alban Desmaison, Luca Antiga, and Adam Lerer. Automatic differentiation in pytorch. *NeurIPS*, 2017.

[34] Hanyu Peng, Jiaxiang Wu, Shifeng Chen, and Junzhou Huang. Collaborative channel pruning for deep networks. In *International Conference on Machine Learning*, pages 5113–5122. PMLR, 2019.

[35] Hanyu Peng, Jiaxiang Wu, Zhiwei Zhang, Shifeng Chen, and Hai-Tao Zhang. Deep network quantization via error compensation. *IEEE Transactions on Neural Networks and Learning Systems*, 2021.

[36] Pramuditha Perera, Ramesh Nallapati, and B. Xiang. Ogan: One-class novelty detection using gans with constrained latent representations. In *2019 IEEE/CVF Conference on Computer Vision and Pattern Recognition (CVPR)*, pages 2893–2901, 2019.

[37] Pramuditha Perera and Vishal M Patel. Learning deep features for one-class classification. *IEEE Transactions on Image Processing*, 28(11):5450–5463, 2019.

[38] Alec Radford, Luke Metz, and Soumith Chintala. Unsupervised representation learning with deep convolutional generative adversarial networks. *CoRR*, abs/1511.06434, 2016.

[39] Adriana Romero, Nicolas Ballas, Samira Ebrahimi Kahou, Antoine Chassang, Carlo Gatta, and Yoshua Bengio. Fitnets: Hints for thin deep nets. *ICLR*, 2015.

[40] Lukas Ruff, Robert Vandermeulen, Nico Goernitz, Lucas Deecke, Shoaib Ahmed Siddiqui, Alexander Binder, Emmanuel Müller, and Marius Kloft. Deep one-class classification. In *International conference on machine learning*, pages 4393–4402, 2018.

[41] Lukas Ruff, Robert A. Vandermeulen, Nico Görnitz, Alexander Binder, E. Müller, K. Müller, and M. Kloft. Deep semi-supervised anomaly detection. In *ICLR*, 2019.

[42] Mohammadreza Salehi, Niousha Sadjadi, Soroosh Baselizadeh, Mohammad H Rohban, and Hamid R Rabiee. Multiresolution knowledge distillation for anomaly detection. In *Proceedings of the IEEE/CVF Conference on Computer Vision and Pattern Recognition*, pages 14902–14912, 2021.

[43] Thomas Schlegl, Philipp Seeböck, Sebastian M Waldstein, Georg Langs, and Ursula Schmidt-Erfurth. f-anogan: Fast unsupervised anomaly detection with generative adversarial networks. *Medical image analysis*, 54:30–44, 2019.

[44] Thomas Schlegl, Philipp Seeböck, Sebastian M. Waldstein, Ursula Schmidt-Erfurth, and Georg Langs. Unsupervised anomaly detection with generative adversarial networks to guide marker discovery. *IPMI*, 2017.

[45] Bernhard Schölkopf, John C. Platt, John Shawe-Taylor, Alexander J. Smola, and Robert C. Williamson. Estimating the support of a high-dimensional distribution. *Neural Computation*, 13(7):1443–1471, 2001.

[46] Abhinav Srivastava, Amlan Kundu, Shamik Sural, and Arun K. Majumdar. Credit card fraud detection using hidden markov model. *IEEE Transactions on Dependable and Secure Computing*, 5(1):37–48, 2008.

[47] Alexander Tong, Guy Wolf, and Smita Krishnaswamy. A lipschitz-constrained anomaly discriminator framework. *ArXiv*, abs/1905.10710, 2019.

[48] S. Venkataraman, K. Peng, Rajat Vikram Singh, and Abhijit Mahalanobis. Attention guided anomaly detection and localization in images. *ArXiv*, abs/1911.08616, 2019.

[49] Pascal Vincent, Hugo Larochelle, Yoshua Bengio, and Pierre-Antoine Manzagol. Extracting and composing robust features with denoising autoencoders. *ICML*, 2008.

[50] Ha Son Vu, D. Ueta, Kiyoshi Hashimoto, K. Maeno, Sugiri Pranata, and S. Shen. Anomaly detection with adversarial dual autoencoders. *ArXiv*, abs/1902.06924, 2019.

[51] Xiaojie Wang, Rui Zhang, Yu Sun, and Jianzhong Qi. Kdgan: knowledge distillation with generative adversarial networks. *NeurIPS*, 2018.

[52] Yunhe Wang, Chang Xu, Chao Xu, and Dacheng Tao. Adversarial learning of portable student networks. *AAAI*, 2018.

[53] Svante Wold, Kim H. Esbensen, and Paul Geladi. Principal component analysis. *Chemometrics and Intelligent Laboratory Systems*, 2(1-3):37–52, 1987.

[54] Peng Wu and Jing Liu. Learning causal temporal relation and feature discrimination for anomaly detection. *IEEE Transactions on Image Processing*, 30:3513–3527, 2021.

[55] Yuxin Wu and Justin Johnson. Rethinking “batch” in batchnorm. *arXiv preprint arXiv:2105.07576*, 2021.

[56] Han Xiao, Kashif Rasul, and Roland Vollgraf. Fashion-mnist: A novel image dataset for benchmarking machine learning. *ArXiv*, abs/1708.07747, 2017.

[57] Houssam Zenati, Chuan Sheng Foo, Bruno Lecouat, Gaurav Manek, and Vijay Ramaseshan Chandrasekhar. Efficient gan-based anomaly detection. *arXiv preprint arXiv:1802.06222*, 2018.